Particulate Oxalate-to-Sulfate Ratio as an Aqueous Processing Marker: Consistency Across Field Campaigns and Limitations

Miguel Ricardo A. Hilario[1], Ewan Crosbie[2,3], Paola Angela Bañaga[4,5], Grace Betito[4,5], Rachel A. Braun[6,†], Maria Obiminda Cambaliza[4,5], Andrea F. Corral[6], Melliza Templonuevo Cruz[4,7], Jack E. Dibb[8], Genevieve Rose Lorenzo[1], Alexander B. MacDonald[6], Claire E. Robinson[2,3], Michael A. Shook[2], James Bernard Simpas[4,5], Connor Stahl[6], Edward Winstead[2,3], Luke D. Ziemba[2], and Armin Sorooshian[1,6]

[1] Department of Hydrology and Atmospheric Sciences, University of Arizona, Tucson, AZ 85721, USA, [2] NASA Langley Research Center, Hampton, VA, USA, [3] Science Systems and Applications, Inc., Hampton, VA, USA, [4] Manila Observatory, Quezon City 1108, Philippines, [5] Department of Physics, School of Science and Engineering, Ateneo de Manila University, Quezon City 1108, Philippines, [6] Department of Chemical and Environmental Engineering, University of Arizona, Tucson, AZ 85721, USA, [7] Institute of Environmental Science and Meteorology, University of the Philippines, Diliman, Quezon City 1101, Philippines, [8] Earth Systems Research Center, Institute for the Study of Earth, Oceans, and Space, University of New Hampshire, Durham, NH, USA

Corresponding author: Armin Sorooshian (`armin@email.arizona.edu`)

[†] Now at: Healthy Urban Environments Initiative, Global Institute of Sustainability and Innovation, Arizona State University, Tempe, AZ, USA

Key Points:

- Multi-campaign consistency in oxalate-sulfate mass ratio 0.0217 (95% confidence interval: $0.0154 - 0.0296$; r = 0.76)

- Oxalate-sulfate mass ratio is biased towards higher values in presence of coarse aerosol particles and/or biomass burning

- Ground-based, size-resolved measurements reveal that the ratio can be robust within the mixed layer for the submicrometer mode

-

Abstract

Leveraging aerosol data from multiple airborne and surface-based field campaigns encompassing diverse environmental conditions, we identify a generally consistent oxalate-sulfate mass ratio, with a median of 0.0217 (95% confidence interval: $0.0154 - 0.0296$; r = 0.76). Ground-based aerosol data show that the median oxalate-sulfate ratio is robust within both the mixed layer and the submicrometer particle size range, with higher values observed for supermicrometer particles. We demonstrate that dust and biomass burning emissions can separately bias this ratio towards higher values by at least one order of magnitude. Since sulfate is more readily measured, this ratio could be used to infer oxalate from sulfate in the absence of biomass burning and/or air masses rich with

coarse aerosol types (especially dust). This ratio may also have implications for model estimates of secondary organic aerosol (SOA) formation, and particularly the aqueous processing route for oxalate production.

Plain Language Summary

In this study, we examined multiple field campaign datasets encompassing a diverse set of environments and identified a consistent oxalate-to-sulfate mass ratio of ~0.02 for aerosol particles. Analysis of ground-based data show that this ratio is robust near the surface for particles below 1 micrometer in diameter. We show that coarse aerosol types, especially dust, and biomass burning particles can bias the oxalate-to-sulfate ratio towards higher values and suggest using the ~0.02 ratio only in their absence. As sulfate is more commonly measured and simulated by models, this finding has implications for model estimates of secondary organic aerosol formation, which is a large source of uncertainty in current chemistry models.

1 Introduction

Organic species account for a major fraction of atmospheric aerosol particles (Hallquist et al., 2009; Kanakidou et al., 2005; Q. Zhang et al., 2007) comprising between $20 - 50\%$ of fine aerosol mass in the continental mid-latitudes (Putaud et al., 2004; Saxena & Hildemann, 1996), 30–80% in the free troposphere (Murphy et al., 2006), and over 80% in tropical forests (Andreae & Crutzen, 1997; Roberts et al., 2001). Secondary organic aerosol (SOA) is derived from gas-to-particle conversion processes, including aqueous processing (Blando & Turpin, 2000; Ervens et al., 2011; Warneck, 2003), wherein oxidized volatile organic compounds (VOCs) partition into cloud droplets or wet aerosol particles and undergo chemical reactions to form low-volatility products that remain in the condensed phase (Ervens, 2015; Ervens et al., 2011; McNeill, 2015). Oxygenated organic species comprise $60 - 95\%$ of total organic aerosol mass across urban and remote sites (Q. Zhang et al., 2007), while SOA from VOCs explains up to 70% of global organic carbon mass (Hallquist et al., 2009). However, despite improvements in modeling organic aerosol (Heald et al., 2005, 2011), atmospheric chemistry models still underestimate SOA (Schroder et al., 2018) due partly to an incomplete understanding and representation of aqueous processes, resulting in poor model parameterization (Hallquist et al., 2009; McNeill, 2015). The inclusion of SOA formation has been shown to decrease model bias (–64% to – 15%) and increase model correlations with observations (r = 0.5 to 0.6) (Carlton et al., 2008); thus, improving SOA estimates is a key area of development for models to more accurately evaluate the impacts of atmospheric aerosol particles and reduce uncertainties regarding the net effect of aerosol particles on health and climate (IPCC, 2014).

Oxalic acid is the most abundant organic acid in tropospheric aerosol particles across different regions (Cruz et al., 2019; Yang et al., 2014; Ziemba et al., 2011) and the dissociated ion oxalate (OXL) is a well-established tracer of aqueous processing, often used in combination with other secondary tracers such as SO_4^{2-}

to assess the extent of aqueous processing in a region (Crahan et al., 2004; Hilario et al., 2020; Sorooshian, Varutbangkul, et al., 2006; G. Wang et al., 2012; Yu et al., 2005). Although minor relative to production via aqueous processing (Ervens, 2015; Huang & Yu, 2007; Myriokefalitakis et al., 2011) and photochemistry (C. Zhang et al., 2020), point sources of OXL include biomass burning (BB) (Narukawa et al., 1999; Yang et al., 2014) and biogenic emissions (Boone et al., 2015). Early model simulations overestimated OXL by an order of magnitude (Crahan et al., 2004) while more recent global simulations by Myriokefalitakis et al. (2011) showed better model estimates over marine/rural environments between observed and modeled OXL (modeled:observed slope = 1.16 ± 0.14; Pearson's r = 0.60) but could not capture OXL over urban regions (weak correlation; r   0).

The OXL:SO_4^{2-} ratio has been suggested in past work to be an indicator of aqueous processing (Ervens et al., 2014; Wonaschuetz et al., 2012; Yu et al., 2005). This implies that OXL and SO_4^{2-} are entirely sourced from aqueous-phase oxidation, whether it be in cloud droplets or wet aerosol particles, and does not account for gas-phase oxidation in cloud-free air (Ervens, 2015). This is a reasonable assumption for SO_4^{2-} given that oxidation in the gas-phase is much slower than in the aqueous-phase (Cautenet & Lefeivre, 1994) and aqueous-phase oxidation explains $60 - 90\%$ of SO_4^{2-} in global models (Barth et al., 2000; Faloona, 2009). Also, there is thought to be no gas-phase source for OXL (Ervens et al., 2014; Warneck, 2003).

Laboratory experiments are often relied on for mechanistic details of aerosol particles (e.g., Hennigan et al., 2010; Pang et al., 2019) but cannot mimic the atmosphere perfectly (May et al., 2014). Thus, aircraft campaigns provide a valuable opportunity to study aerosol particles influenced by cloud processes in their most natural environment (Sorooshian et al., 2020). This study leverages composition data from multiple field campaigns, predominantly based on airborne measurements, to investigate the following questions: (1) Is there a generally consistent range of OXL:SO_4^{2-} across different regions?; (2) is there a size dependence of this ratio?; and (3) under what conditions does the OXL:SO_4^{2-} relationship break down?

2 Methods

This work relies mostly on airborne field datasets, with the focus predominantly being on particle-into-liquid sampler (PILS) data. The PILS grows sampled aerosol particles into droplets sufficiently large to be collected via inertial impaction, with the resultant liquid transported to vials on a rotating carousel for post-collection chemical analysis via ion chromatography (IC) (Sorooshian, Brechtel, et al., 2006; Weber et al., 2001). While most attention is given to the Cloud, Aerosol, and Monsoon Processes-Philippines Experiment (CAMP²Ex), broader context is provided from a variety of other datasets. Continental data are used from the International Consortium for Atmospheric Research on Transport and Transformation (ICARTT; August 2004; < 3 km AGL) over the Ohio River Valley, USA (Fehsenfeld et al., 2006; Sorooshian, Varutbangkul, et al.,

2006) and the Gulf of Mexico Atmospheric Composition and Climate Study (Go-MACCS; August – September 2006; < 5 km AGL) over Texas, USA (Parrish et al., 2009; Sorooshian, Ng, et al., 2007). Marine/coastal data were collected over the Northeast Pacific Ocean from the following campaigns (Sorooshian et al., 2018): the Marine Stratus/Stratocumulus Experiment (MASE-I; July 2005; < 3.5 km AGL) (Lu et al., 2007; Sorooshian, Lu, et al., 2007), the Marine Stratus/Stratocumulus Experiment II (MASE-II; July 2007; < 2.5 km AGL) (Lu et al., 2009; Sorooshian et al., 2009), and (3) the Nucleation in California Experiment (NiCE; July – August 2013; < 3 km AGL) (Sorooshian et al., 2015). We also include marine/coastal data over different oceanic basins: CAMP^{2}Ex (August – October 2019; < 9 km AGL) over the West Pacific (Hilario et al., 2021), the Aerosol Cloud meTeorology Interactions oVer the western ATlantic Experiment (ACTIVATE; August – September 2020; < 5 km AGL) over the western North Atlantic Ocean (Sorooshian et al., 2019), and the Atmospheric Tomography Mission (AToM; 2016 – 2018; < 12 km AGL) over the Pacific (50 °S to 50 °N; 155 °E to 235 °E) and Atlantic (50 °S to 50 °N; 310 °E to 0 °E) Oceans (Wofsy et al., 2018). AToM OXL and SO_4^{2-} were collected by Soluble Acidic Gases and Aerosol (SAGA) filters (Dibb et al., 2002, 2003).

To evaluate both the size-dependence and mixed layer values of the OXL:SO_4^{2-} ratio, we included ground-based data collected by a micro-orifice uniform deposit impactor (MOUDI) and analyzed via IC during the CAMP^{2}Ex weatHEr and CompoSition Monitoring (CHECSM; July 2018 – October 2019; 85 m AGL) campaign in Metro Manila, Philippines (Cruz et al., 2019; Stahl, Cruz, Bañaga, Betito, Braun, Aghdam, Cambaliza, Lorenzo, MacDonald, Pabroa, et al., 2020). We specifically examined a total of 53 MOUDI sets that were collected on a weekly basis with a sample duration of ~48 hours per set. Six of those sets were impacted by BB based on the criteria presented by Gonzalez et al. (2021) for the same dataset.

In addition to the PILS, we analyze submicrometer non-refractory aerosol from the aerosol mass spectrometer (AMS; Aerodyne) (Canagaratna et al., 2007; De-Carlo et al., 2006) from CAMP^{2}Ex. A comparison of SO_4^{2-} from the PILS and AMS at CAMP^{2}Ex shows good agreement (AMS:PILS slope = 0.81; r = 0.88), suggesting that SO_4^{2-} at CAMP^{2}Ex was predominantly in the submicrometer size range given the size ranges of the AMS (PM_1) and PILS ($PM_{\sim4}$). Furthermore, a calculation of sea-salt SO_4^{2-} using the ratio of SO_4^{2-} and Na^+ for pure sea salt reveals that on average less than 5% of SO_4^{2-} at CAMP^{2}Ex was from sea salt.

Multiple campaigns (ICARTT, GoMACCS, MASE-I, MASE-II, NiCE) collected PM_1 except for CAMP^{2}Ex ($PM_{\sim4}$), ACTIVATE ($PM_{\sim4}$), AToM ($PM_{\sim4}$) and CHECSM (0.056 – 18 m; PM_{18}), which included contributions from coarse mode particles. For AToM, CAMP^{2}Ex, and ACTIVATE, the aerosol sampling inlet likely limits the upper size to approximately 4 m (McNaughton et al., 2007) although there may be some additional impaction losses in the sampling lines internal to the aircraft that may further smooth the particle transmission curve

near this upper bound. This higher cutoff size allowed for sampling of sea salt and dust. To meaningfully compare $OXL:SO_4^{2-}$ ratios between campaigns, we separated out samples impacted by strong point sources (e.g., ship plumes, cattle feedlots, smoke) as identified using flight scientist notes and clear enhancements in particle concentration data.

In this study, the $OXL:SO_4^{2-}$ ratio refers to the regression slope derived via least-squares. When calculating species ratios (Table 1), we excluded instances when the denominator value was below its 5th percentile to reduce the uncertainty caused by low denominator values. Ratios in this study refer to mass ratios unless otherwise indicated (e.g., molar ratios). To quantify an all-campaign statistic and uncertainty, median and 95% confidence intervals of the $OXL:SO_4^{2-}$ ratio were derived via bootstrapping over different combinations of sample size and number of iterations, excluding samples with confounding influence (further details are provided in Table S1).

3 Results

3.1. Consistency in the $OXL:SO_4^{2-}$ Ratio

Across multiple environments (Fig. 1), we observe overall agreement in the $OXL:SO_4^{2-}$ ratio (i.e., slope) across campaigns except for $CAMP^2Ex$ (discussed in Section 3.2). Bootstrapping reveals a stable median $OXL:SO_4^{2-}$ of 0.0217 (95% confidence interval: 0.0154 – 0.0296; r = 0.76) (details in Table S1). This is supported by averaging the $OXL:SO_4^{2-}$ ratios between campaigns in Fig. 1 (mean: 0.0184, standard deviation: 0.007, median absolute deviation (MAD): 0.004). Correlation coefficients below 0.50 (Fig. 1) signify the presence of confounding sources of OXL and/or SO_4^{2-}, an expected result given the diversity of environments analyzed; this was especially evident from $CAMP^2Ex$, which is the subject of the subsequent sections. Variability in ratios between campaigns may be partly suggestive of SO_4^{2-} from cloud-free photochemistry (Ervens, 2015). Considering the differences between OXL and SO_4^{2-} in terms of their precursors, formation mechanisms, and sinks, the general stability of the $OXL:SO_4^{2-}$ ratio across multiple environments implies a convergence towards a fairly narrow range, which is assisted in part by the large sample sizes used in this study.

The ground-based CHECSM ratio (PM_{18}: 0.0264; PM_1: 0.0196; r = 0.73 for both size ranges) falls within the 95% confidence interval in the absence of BB (Fig. 1f), particularly between 0.32–1 m (Fig. S1a) where most of the OXL and SO_4^{2-} mass resides (Cruz et al., 2019). This suggests that the ratio applies to the mixed layer. The increase in $OXL:SO_4^{2-}$ in the supermicrometer range suggests the enhancement of OXL via partitioning onto coarse particles as documented for the study region (Stahl, Cruz, Bañaga, Betito, Braun, Aghdam, Cambaliza, Lorenzo, MacDonald, Hilario, et al., 2020). Considering most campaigns in this study sampled PM_1, the size-resolved results from CHECSM imply that our $OXL:SO_4^{2-}$ value of 0.0217 may primarily be a submicrometer characteristic.

With its global coverage of tropospheric aerosol concentrations, the AToM campaign provides insight into the $OXL:SO_4^{2-}$ ratio over remote marine environ-

5

ments in both hemispheres. Below 3 km AGL, the Pacific and Atlantic Oceans have an OXL:SO_4^{2-} ratio of 0.0207 (r = 0.51) (Fig. 1g). Separately, the Pacific and Atlantic have ratios of 0.0180 (r = 0.36) and 0.0251 (r = 0.72), respectively, which is remarkably similar to other environments in Fig. 1. A comparison across altitudes and latitudes (Fig. S2) reveals that the ratio for the Pacific from the surface to as high as 7.5 km AGL is within our 95% confidence interval (Fig. S2a) but only near-surface Atlantic samples fall within our confidence interval (Fig. S2c), possibly due to OXL partitioning onto Saharan dust. Similar findings from CAMP²Ex will be discussed in Section 3.2.

For comparison, past studies reported the following values of OXL:SO_4^{2-}:.036 in urban/coastal Hong Kong ($PM_{2.5}$; r = 0.89) (Yao et al., 2004), 0.037 in coastal Canada (total suspended particles; r = 0.83) (Liu et al., 1996), and 0.049 from East Asian aircraft samples (PM_7; r = 0.85) (Mader et al., 2004). Yu et al. (2005) reported $PM_{2.5}$ OXL:SO_4^{2-} in the following regions (in mass ratio units): summertime Beijing (0.0174, r = 0.95), Pearl River Delta region (0.0238, r = 0.87), Nanjing in the fall (0.0266, r = 0.84) and winter (0.0156, r = 0.84). There is some similarity with our values and, as will be shown, coarse aerosol particles can bias the ratio to higher values consistent with some of the aforementioned studies sampling well above 1 µm.

6
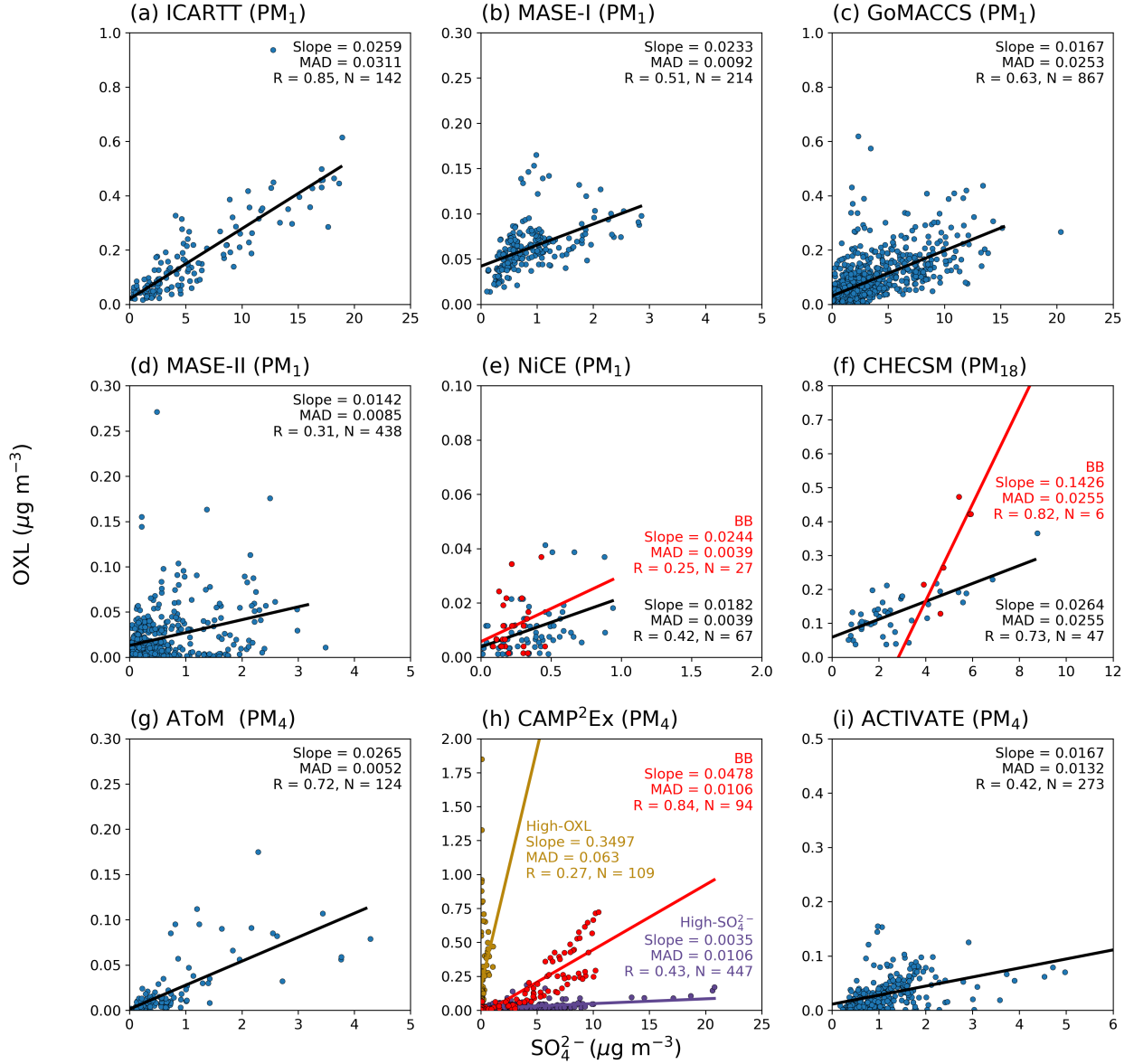
Figure 1. Linear regressions of OXL and SO_4^{2-} across different field campaigns. All campaigns are aircraft-based except for CHECSM, which was ground-based. Statistics for BB-impacted samples are presented separately in red. $CAMP^2Ex$ high-OXL and high-SO_4^{2-} populations are colored in yellow and purple, respectively, in (h). Axes limits are not standardized across panels. In addition to Pearson's R, the median absolute deviation (MAD) was used as a measure of slope goodness-of-fit.

3.2. Source of the CAMP^{2}Ex high-OXL population

Oxalate and $SO_4{}^{2-}$ from CAMP^{2}Ex show three populations: high-OXL, high-$SO_4{}^{2-}$, and BB-impacted, each characterized by a distinct $OXL{:}SO_4{}^{2-}$ slope (Fig. 1a). BB-impacted samples are defined as data collected during RFs 9 and 10 (15 and 16 September 2019, respectively), which targeted smoke emissions. The high-OXL population was defined with $OXL{:}SO_4{}^{2-} > 0.3$ and the high-$SO_4{}^{2-}$ population with $OXL{:}SO_4{}^{2-} < 0.06$; varying the high-OXL ratio lower threshold within $0.10 - 0.30$ and high-$SO_4{}^{2-}$ upper threshold within $0.06 - 0.10$ does not impact results of the analyses presented below. Ensuing discussion about these three populations points to important influences on the $OXL{:}SO_4{}^{2-}$ ratio.

The high-OXL population during CAMP^{2}Ex (Fig. 1h) was not observed in the other field campaigns. These high-OXL samples were mostly sampled within the free troposphere (> 5 km) (Fig. S3b), altitudes of which were rarely sampled in other field campaigns with AToM being the exception. A few reasons can explain the high-altitude, high-OXL samples: (1) OXL's lengthier chemical formation pathways compared to $SO_4{}^{2-}$ (Ervens, 2015; Sorooshian, Lu, et al., 2007), (2) inefficient scavenging of gaseous precursors as air masses are transported upward (Heald et al., 2005), and (3) OXL partitioning onto dust particles (Stahl, Cruz, Bañaga, Betito, Braun, Aghdam, Cambaliza, Lorenzo, MacDonald, Hilario, et al., 2020; Sullivan & Prather, 2007). As the PILS sampled PM_4 during CAMP^{2}Ex, we hypothesize that the enhanced OXL is due to the partitioning of OXL precursors onto coarse mode particles such as dust or sea salt (Mochida et al., 2003; Rinaldi et al., 2011; Sullivan & Prather, 2007; Turekian et al., 2003). Among the two sources, dust is more likely based on OXL's higher affinity for it compared to sea salt (Stahl, Cruz, Bañaga, Betito, Braun, Aghdam, Cambaliza, Lorenzo, MacDonald, Hilario, et al., 2020). Furthermore, efficient wet scavenging of sea salt reduces its free troposphere concentrations as compared to those of the marine boundary layer (Murphy et al., 2019; Schlosser et al., 2020).

To more deeply characterize the high-OXL population, we compared several key variables between the CAMP^{2}Ex high-OXL and high-$SO_4{}^{2-}$ populations (Table 1), all of which showed statistically significant differences based on the Mann-Whitney U-test (99% confidence level; $p < 0.01$). The following characteristics hint to the partitioning of OXL onto dust aloft: (1) dust species such as Ca^{2+} (Kchih et al., 2015) had approximately double the mass concentration in high-OXL air as compared to high-$SO_4{}^{2-}$ air (Table 1), (2) high-OXL air was mostly sampled in the free troposphere (Fig. S3), (3) ionic crustal ratios in the free troposphere (> 5 km) were more similar to dust values than those for sea salt based on literature (Park et al., 2004; Švédová et al., 2019; Q. Wang et al., 2018) (Fig. 2). For the other two campaigns sampling PM_4, elevated $OXL{:}SO_4{}^{2-}$ at higher altitudes were also observed during AToM (Fig. S2), whereas during ACTIVATE, dust was not prevalent at the altitudes sampled (0–5 km).

We next compared m/z 44_{AMS} and OXL (from PILS) to assess the possibility of OXL partitioning onto coarse mode particles such as dust. m/z 44_{AMS} indicates the mass concentration of oxygenated/aged organic aerosol with the functional

group CO_2^+ (Qi Zhang et al., 2005), of which OXL is a subcomponent. As the AMS sampled PM_1 and the PILS sampled PM_4 in $CAMP^2Ex$, their comparison lends insight into how coarse mode particles (i.e., 1–4 m) bias PILS observations. Furthermore, because OXL is one component of m/z 44_{AMS}, comparing PILS OXL (PM_4) to m/z 44_{AMS} (PM_1) can serve as an indicator of coarse mode OXL if OXL:m/z 44_{AMS} 1 as a highly conservative threshold. The high-OXL population has an OXL:m/z 44_{AMS} molar ratio of 2.84 ± 3.95 (Table 1), which provides strong evidence for coarse mode OXL (1–4 m). This is supported by a high OXL:Org_{AMS} ratio in the high-OXL population (0.84 ± 0.98) compared to the high-SO_4^{2-} population (0.01 ± 0.01). Interestingly, Org_{AMS}:$SO_4^{2-}{}_{AMS}$ is similar between the high-OXL (1.08 ± 1.34) and high-SO_4^{2-} populations (1.27 ± 1.02). Since the AMS samples PM_1, these findings offer more evidence that differences between populations lie in the coarse mode.

Table 1. Bulk statistics (mean ± standard deviation) comparing high-OXL and high-SO_4^{2-} populations from $CAMP^2Ex$. Number of samples are included in parentheses. All variables exhibit statistically significant differences between populations (Mann-Whitney U-test; $p < 0.01$). The rightmost column presents values from the high-OXL column divided by those in the high-SO_4^{2-} column to compare the two populations more directly. Rows are arranged in descending order of the ratio column (i.e., decreasing from top to bottom). Variables marked by * were cloud-screened to remove potential sampling artifacts related to droplet shatter. Ratios between species were not cloud-screened as ratios are assumed to be conserved regardless of sampling conditions. Note that OXL:$m/z44_{AMS}$ is presented as a molar ratio as we assume every OXL molecule produces a CO_2^+ ion in the AMS.

	High-OXL	High-SO_4^{2-}	Ratio
Oxalate:Org_{AMS}	0.84 ± 0.98 (41)	0.01 ± 0.01 (401)	71.58 ± 120.42
Oxalate:$m/z44_{AMS}$	2.84 ± 3.95 (102)	0.04 ± 0.06 (425)	34.42 ± 138.67
Oxalate (g m^{-3})*	0.25 ± 0.27 (83)	0.03 ± 0.03 (343)	10.21 ± 14.83
Ca^{2+}:Na^+	3.57 ± 4.06 (36)	0.39 ± 0.95 (312)	9.08 ± 24.24
K^+:Na^+	1.75 ± 4.07 (32)	0.20 ± 0.54 (224)	8.68 ± 30.79
Mg^{2+}:Na^+	0.73 ± 0.58 (32)	0.11 ± 0.10 (323)	6.42 ± 7.77
Ca^{2+} (g m^{-3})*	0.20 ± 0.26 (45)	0.09 ± 0.13 (260)	2.25 ± 4.42
Ca^{2+}:Mg^{2+}	6.11 ± 4.78 (47)	3.16 ± 4.44 (276)	1.93 ± 3.11
Org_{AMS}:$SO_4^{2-}{}_{AMS}$	1.08 ± 1.34 (90)	1.27 ± 1.02 (425)	0.85 ± 1.26
Na^+ (g m^{-3})*	0.08 ± 0.08 (35)	0.41 ± 0.43 (292)	0.20 ± 0.30
SO_4^{2-} (g m^{-3})*	0.20 ± 0.25 (83)	3.12 ± 2.89 (343)	0.07 ± 0.10
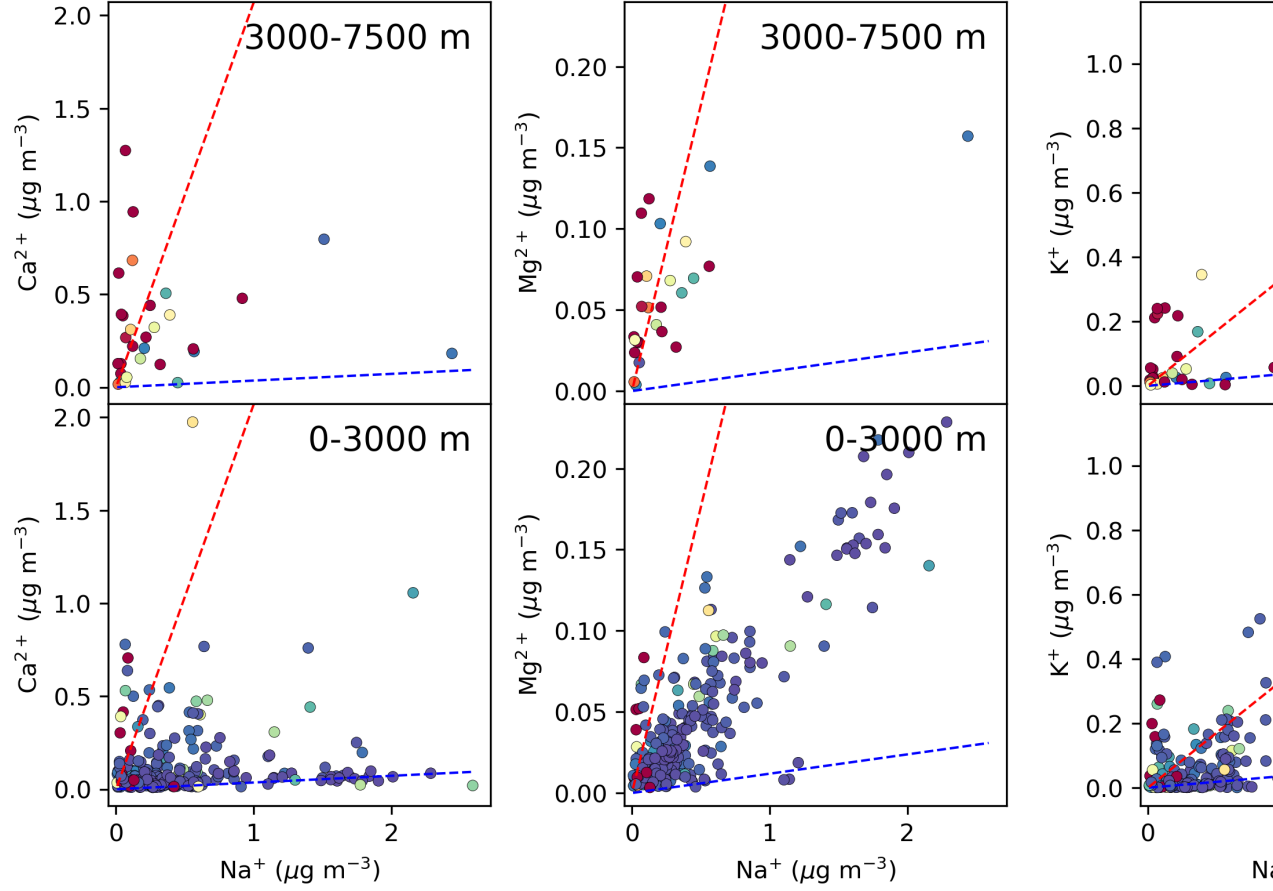
Figure 2. Altitude-resolved linear regressions of PILS dust species during $CAMP^2Ex$ (BB samples excluded) colored by $OXL:SO_4^{2-}$. Red and blue dashed lines denote literature-based ratios for dust (Park et al., 2004; Švédová et al., 2019; Q. Wang et al., 2018) and sea salt (Chesselet et al., 1972), respectively.

3.3. Impact of biomass burning on $OXL:SO_4^{2-}$

Although strong OXL and SO_4^{2-} correlations may be interpreted as a signal of aqueous processing (Sorooshian, Varutbangkul, et al., 2006; Yao et al., 2003; Yu et al., 2005), the presence of BB emissions must also be considered as a source of both SO_4^{2-} and OXL (Narukawa et al., 1999; Yang et al., 2014). When present, BB emissions led to enhanced $OXL:SO_4^{2-}$ ratios and correlations (Fig. 1). Similar enhancements were observed during CHECSM for BB-impacted, size-resolved $OXL:SO_4^{2-}$ (Fig. S1b). Differences in BB-related $OXL:SO_4^{2-}$ between campaigns may be attributed to factors including biomass type (Christian et al., 2003), wet scavenging during transport (Marelle et al., 2015), combustion phase (Kondo et al., 2011; Pósfai et al., 2003), and sampled size range (i.e.,

PM_4 for CAMP^{2}Ex, PM_1 for NiCE, PM_{18} for CHECSM). During CAMP^{2}Ex, BB-impacted data suggested two subpopulations that differ slightly in their OXL:SO$_4^{2-}$ slopes (Fig. 1h). Both populations were sampled during a large biomass burning event (15 Sep 2019; RF9) but differ in terms of location (~330 km apart), composition, and number concentration (not shown), pointing to clear differences within the CAMP^{2}Ex BB-impacted population left for future work. Regardless of BB differences between campaigns, such a pronounced impact on the OXL:SO$_4^{2-}$ ratio in those respective datasets demonstrates the importance of accounting for BB when exploiting the OXL:SO$_4^{2-}$ ratio for analysis and modeling purposes relevant to secondary aerosol formation processes.

4 Conclusions

Using composition data from multiple campaigns spanning a variety of environments, we identified a generally consistent OXL:SO$_4^{2-}$ mass ratio (median: 0.0217; 95% confidence interval: 0.0154 – 0.0296; r = 0.76). Environments include continental and coastal North America; west, east, and central Pacific Ocean; and west and central Atlantic Ocean. The median ratio is proposed to be robust relative to a wide range of factors that can impact the formation and removal of both OXL and SO$_4^{2-}$ owing to the large sample sets used and data coverage over marine and continental regions encompassing a wide range of pollution sources and cloud fractions. Ground-based size-resolved measurements show overall agreement with the proposed ratio, specifically within the submicrometer mode, suggesting the ratio is robust within the mixed layer for PM$_1$. Enhanced OXL:SO$_4^{2-}$ during CAMP^{2}Ex was associated with OXL partitioning onto dust in the free troposphere. Additionally, BB emissions as a source of both OXL and SO$_4^{2-}$ may produce a strong correlation and bias their ratio towards higher values. Thus, we caution against interpretating a strong OXL and SO$_4^{2-}$ correlation as a standalone signature of aqueous processing when coarse particle types and/or BB emissions are present.

Given its consistency across different environments, the median OXL:SO$_4^{2-}$ ratio of 0.0217 could have implications for model estimates of aqueous processing. Future work is encouraged to assess the use of this OXL:SO$_4^{2-}$ ratio to estimate aqueous processing in models. Examining the OXL:SO$_4^{2-}$ ratio in other parts of the world and seasons would also be beneficial to gauge its variability as well as to identify other potentially confounding factors. In particular, the on-going and multi-seasonal ACTIVATE campaign will provide a valuable dataset for future investigations of this nature.

References

Andreae, M. O., & Crutzen, P. J. (1997). Atmospheric Aerosols: Biogeochemical Sources and Role in Atmospheric Chemistry. *Science*, *276*(5315), 1052–1058. https://doi.org/10.1126/science.276.5315.1052Barth, M. C., Rasch, P. J., Kiehl, J. T., Benkovitz, C. M., & Schwartz, S. E. (2000). Sulfur chemistry in the National Center for Atmospheric Research Community Climate Model: Description, evaluation, features, and sensitivity to aqueous chemistry. *Journal of Geophysical Research: Atmospheres*, *105*(D1), 1387–1415. https://doi.org/10.1029/1999JD900773Blando, J. D., & Turpin, B. J. (2000). Secondary organic aerosol formation in cloud and fog droplets: a literature evaluation of plausibility. *Atmospheric Environment*, *34*(10), 1623–1632. https://doi.org/10.1016/S1352-2310(99)00392-1Boone, E. J., Laskin, A., Laskin, J., Wirth, C., Shepson, P. B., Stirm, B. H., & Pratt, K. A. (2015). Aqueous Processing of Atmospheric Organic Particles in Cloud Water Collected via Aircraft Sampling. *Environmental Science & Technology*, *49*(14), 8523–8530. https://doi.org/10.1021/acs.est.5b01639Canagaratna, M. R., Jayne, J. T., Jimenez, J. L., Allan, J. D., Alfarra, M. R., Zhang, Q., et al. (2007). Chemical and microphysical characterization of ambient aerosols with the aerodyne aerosol mass spectrometer. *Mass Spectrometry Reviews*, *26*(2), 185–222. https://doi.org/10.1002/mas.20115Carlton, A. G., Turpin, B. J., Altieri, K. E., Seitzinger, S. P., Mathur, R., Roselle, S. J., & Weber, R. J. (2008). CMAQ Model Performance Enhanced When In-Cloud Secondary Organic Aerosol is Included: Comparisons of Organic Carbon Predictions with Measurements. *Environmental Science & Technology*, *42*(23), 8798–8802. https://doi.org/10.1021/es801192nCautenet, S., & Lefeivre, B. (1994). Contrasting behavior of gas and aerosol scavenging in convective rain: A numerical and experimental study in the African equatorial forest. *Journal of Geophysical Research: Atmospheres*, *99*(D6), 13013–13024. https://doi.org/10.1029/93JD02712Chesselet, R., Morelli, J., & Buat-Menard, P. (1972). Variations in ionic ratios between reference sea water and marine aerosols. *Journal of Geophysical Research (1896-1977)*, *77*(27), 5116–5131.

https://doi.org/10.1029/JC077i027p05116Christian, T. J., Kleiss, B., Yokelson, R., Holzinger, R., & Crutzen, P. J. (2003). Comprehensive laboratory measurements of biomass-burning emissions: 1. Emissions from Indonesian, African, and other fuels. *Journal of Geophysical Research*, *108*(D23), 4719. https://doi.org/10.1029/2003JD003704Crahan, K. K., Hegg, D., Covert, D. S., & Jonsson, H. (2004). An exploration of aqueous oxalic acid production in the coastal marine atmosphere. *Atmospheric Environment*, *38*(23), 3757–3764. https://doi.org/10.1016/j.atmosenv.2004.04.009Cruz, M. T., Bañaga, P. A., Betito, G., Braun, R. A., Stahl, C., Aghdam, M. A., et al. (2019). Size-resolved composition and morphology of particulate matter during the southwest monsoon in Metro Manila, Philippines. *Atmospheric Chemistry and Physics*, *19*(16), 10675–10696. https://doi.org/10.5194/acp-19-10675-2019DeCarlo, P. F., Kimmel, J. R., Trimborn, A., Northway, M. J., Jayne, J. T., Aiken, A. C., et al. (2006). Field-deployable, high-resolution, time-of-flight aerosol mass spectrometer. *Analytical Chemistry*, *78*(24), 8281–8289. https://doi.org/10.1021/ac061249nDibb, J. E., Talbot, R. W., Seid, G., Jordan, C., Scheuer, E., Atlas, E., et al. (2002). Airborne sampling of aerosol particles: Comparison between surface sampling at Christmas Island and P-3 sampling during PEM-Tropics B. *Journal of Geophysical Research: Atmospheres*, *107*(D2), PEM 2-1-PEM 2-17. https://doi.org/10.1029/2001JD000408Dibb, J. E., Talbot, R. W., Scheuer, E. M., Seid, G., Avery, M. A., & Singh, H. B. (2003). Aerosol chemical composition in Asian continental outflow during the TRACE-P campaign: Comparison with PEM-West B. *Journal of Geophysical Research: Atmospheres*, *108*(D21). https://doi.org/10.1029/2002JD003111Ervens, B. (2015). Modeling the Processing of Aerosol and Trace Gases in Clouds and Fogs. *Chem. Rev.*, 42.Ervens, B., Turpin, B. J., & Weber, R. J. (2011). Secondary organic aerosol formation in cloud droplets and aqueous particles (aqSOA): a review of laboratory, field and model studies. *Atmospheric Chemistry and Physics*, *11*(21), 11069–11102. https://doi.org/10.5194/acp-11-11069-2011Ervens, B., Sorooshian, A., Lim, Y. B., & Turpin, B. J. (2014). Key parameters controlling OH-initiated formation of secondary organic aerosol in the aqueous phase (aqSOA). *Journal of Geophysical Research: Atmospheres*, *119*(7), 3997–4016. https://doi.org/10.1002/2013JD021021Faloona, I. (2009). Sulfur processing in the marine atmospheric boundary layer: A review and critical assessment of modeling uncertainties. *Atmospheric Environment*, *43*(18), 2841–2854. https://doi.org/10.1016/j.atmosenv.2009.02.043Fehsenfeld, F. C., Ancellet, G., Bates, T. S., Goldstein, A. H., Hardesty, R. M., Honrath, R., et al. (2006). International Consortium for Atmospheric Research on Transport and Transformation (ICARTT): North America to Europe-Overview of the 2004 summer field study. *Journal of Geophysical Research: Atmospheres*, *111*(D23). https://doi.org/10.1029/2006JD007829Gonzalez, M. E., Stahl, C., Cruz, M. T., Bañaga, P. A., Betito, G., Braun, R. A., et al. (2021). Contrasting the size-resolved nature of particulate arsenic, cadmium, and lead among diverse regions. *Atmospheric Pollution Research*, *12*(3), 352–361. https://doi.org/10.1016/j.apr.2021.01.002Hallquist, M., Wenger, J. C., Baltensperger, U., Rudich, Y., Simpson, D., Claeys,

M., et al. (2009). The formation, properties and impact of secondary organic aerosol: current and emerging issues. *Atmospheric Chemistry and Physics*, *9*(14), 5155–5236. https://doi.org/10.5194/acp-9-5155-2009Heald, C. L., Jacob, D. J., Park, R. J., Russell, L. M., Huebert, B. J., Seinfeld, J. H., et al. (2005). A large organic aerosol source in the free troposphere missing from current models. *Geophysical Research Letters*, *32*(18). https://doi.org/10.1029/2005GL023831Heald, C. L., Coe, H., Jimenez, J. L., Weber, R. J., Bahreini, R., Middlebrook, A. M., et al. (2011). Exploring the vertical profile of atmospheric organic aerosol: comparing 17 aircraft field campaigns with a global model. *Atmospheric Chemistry and Physics*, *11*(24), 12673–12696. https://doi.org/10.5194/acp-11-12673-2011Hennigan, C. J., Sullivan, A. P., Collett, J. L., & Robinson, A. L. (2010). Levoglucosan stability in biomass burning particles exposed to hydroxyl radicals. *Geophysical Research Letters*, *37*(9). https://doi.org/10.1029/2010GL043088Hilario, M. R. A., Cruz, M. T., Bañaga, P. A., Betito, G., Braun, R. A., Stahl, C., et al. (2020). Characterizing weekly cycles of particulate matter in a coastal megacity: The importance of a seasonal, size-resolved, and chemically-speciated analysis. *Journal of Geophysical Research: Atmospheres.* https://doi.org/10.1029/2020JD032614Hilario, M. R. A., Crosbie, E., Shook, M., Reid, J. S., Cambaliza, M. O. L., Simpas, J. B. B., et al. (2021). Measurement report: Long-range transport patterns into the tropical northwest Pacific during the CAMP^{2}Ex aircraft campaign: chemical composition, size distributions, and the impact of convection. *Atmospheric Chemistry and Physics*, *21*(5), 3777–3802. https://doi.org/10.5194/acp-21-3777-2021Huang, X.-F., & Yu, J. Z. (2007). Is vehicle exhaust a significant primary source of oxalic acid in ambient aerosols? *Geophysical Research Letters*, *34*(2). https://doi.org/10.1029/2006GL028457Intergovernmental Panel on Climate Change. (2014). *Climate Change 2014 Mitigation of Climate Change: Working Group III Contribution to the Fifth Assessment Report of the Intergovernmental Panel on Climate Change.* Cambridge: Cambridge University Press. https://doi.org/10.1017/CBO9781107415416Kanakidou, M., Seinfeld, J. H., Pandis, S. N., Barnes, I., Dentener, F. J., Facchini, M. C., et al. (2005). Organic aerosol and global climate modelling: a review. *Atmospheric Chemistry and Physics*, *5*(4), 1053–1123. https://doi.org/10.5194/acp-5-1053-2005Kchih, H., Perrino, C., & Cherif, S. (2015). Investigation of Desert Dust Contribution to Source Apportionment of PM10 and PM2.5 from a Southern Mediterranean Coast. *Aerosol and Air Quality Research*, *15*(2), 454–464. https://doi.org/10.4209/aaqr.2014.10.0255Kondo, Y., Matsui, H., Moteki, N., Sahu, L., Takegawa, N., Kajino, M., et al. (2011). Emissions of black carbon, organic, and inorganic aerosols from biomass burning in North America and Asia in 2008. *Journal of Geophysical Research*, *116*(D8), D08204. https://doi.org/10.1029/2010JD015152Liu, P. S. K., Leaitch, W. R., Banic, C. M., Li, S.-M., Ngo, D., & Megaw, W. J. (1996). Aerosol observations at Chebogue Point during the 1993 North Atlantic Regional Experiment: Relationships among cloud condensation nuclei, size distribution, and chemistry. *Journal of Geophysical Research: Atmospheres*, *101*(D22), 28971–28990.

https://doi.org/10.1029/96JD00445Lu, M.-L., Conant, W. C., Jonsson, H. H., Varutbangkul, V., Flagan, R. C., & Seinfeld, J. H. (2007). The Marine Stratus/Stratocumulus Experiment (MASE): Aerosol-cloud relationships in marine stratocumulus. *Journal of Geophysical Research: Atmospheres*, *112*(D10). https://doi.org/10.1029/2006JD007985Lu, M.-L., Sorooshian, A., Jonsson, H. H., Feingold, G., Flagan, R. C., & Seinfeld, J. H. (2009). Marine stratocumulus aerosol-cloud relationships in the MASE-II experiment: Precipitation susceptibility in eastern Pacific marine stratocumulus. *Journal of Geophysical Research*, *114*(D24), D24203. https://doi.org/10.1029/2009JD012774Mader, B. T., Yu, J. Z., Xu, J. H., Li, Q. F., Wu, W. S., Flagan, R. C., & Seinfeld, J. H. (2004). Molecular composition of the water-soluble fraction of atmospheric carbonaceous aerosols collected during ACE-Asia. *Journal of Geophysical Research: Atmospheres*, *109*(D6). https://doi.org/10.1029/2003JD004105Marelle, L., Raut, J.-C., Thomas, J. L., Law, K. S., Quennehen, B., Ancellet, G., et al. (2015). Transport of anthropogenic and biomass burning aerosols from Europe to the Arctic during spring 2008. *Atmospheric Chemistry and Physics*, *15*(7), 3831–3850. https://doi.org/10.5194/acp-15-3831-2015May, A. A., McMeeking, G. R., Lee, T., Taylor, J. W., Craven, J. S., Burling, I., et al. (2014). Aerosol emissions from prescribed fires in the United States: A synthesis of laboratory and aircraft measurements. *Journal of Geophysical Research: Atmospheres*, *119*(20), 11,826-11,849. https://doi.org/10.1002/2014JD021848McNaughton, C. S., Clarke, A. D., Howell, S. G., Pinkerton, M., Anderson, B., Thornhill, L., et al. (2007). Results from the DC-8 Inlet Characterization Experiment (DICE): Airborne Versus Surface Sampling of Mineral Dust and Sea Salt Aerosols. *Aerosol Science and Technology*, *41*(2), 136–159. https://doi.org/10.1080/02786820601118406McNeill, V. F. (2015). Aqueous Organic Chemistry in the Atmosphere: Sources and Chemical Processing of Organic Aerosols. *Environmental Science & Technology*, *49*(3), 1237–1244. https://doi.org/10.1021/es5043707Mochida, M., Kawabata, A., Kawamura, K., Hatsushika, H., & Yamazaki, K. (2003). Seasonal variation and origins of dicarboxylic acids in the marine atmosphere over the western North Pacific. *Journal of Geophysical Research*, *108*(D6), 4193. https://doi.org/10.1029/2002JD002355Murphy, D. M., Cziczo, D. J., Froyd, K. D., Hudson, P. K., Matthew, B. M., Middlebrook, A. M., et al. (2006). Single-particle mass spectrometry of tropospheric aerosol particles. *Journal of Geophysical Research: Atmospheres*, *111*(D23). https://doi.org/10.1029/2006JD007340Murphy, D. M., Froyd, K. D., Bian, H., Brock, C. A., Dibb, J. E., DiGangi, J. P., et al. (2019). The distribution of sea-salt aerosol in the global troposphere. *Atmospheric Chemistry and Physics*, *19*(6), 4093–4104. https://doi.org/10.5194/acp-19-4093-2019Myriokefalitakis, S., Tsigaridis, K., Mihalopoulos, N., Sciare, J., Nenes, A., Kawamura, K., et al. (2011). In-cloud oxalate formation in the global troposphere: a 3-D modeling study. *Atmospheric Chemistry and Physics*, *11*(12), 5761–5782. https://doi.org/10.5194/acp-11-5761-2011Narukawa, M., Kawamura, K., Takeuchi, N., & Nakajima, T. (1999). Distribution of dicarboxylic acids and carbon isotopic compositions in aerosols

from 1997 Indonesian forest fires. *Geophysical Research Letters*, *26*(20), 3101–3104. https://doi.org/10.1029/1999GL010810Orsini, D. A., Ma, Y., Sullivan, A., Sierau, B., Baumann, K., & Weber, R. J. (2003). Refinements to the particle-into-liquid sampler (PILS) for ground and airborne measurements of water soluble aerosol composition. *Atmospheric Environment*, *37*(9), 1243–1259. https://doi.org/10.1016/S1352-2310(02)01015-4Pang, H., Zhang, Q., Wang, H., Cai, D., Ma, Y., Li, L., et al. (2019). Photochemical Aging of Guaiacol by Fe(III)–Oxalate Complexes in Atmospheric Aqueous Phase. *Environmental Science & Technology*, *53*(1), 127–136. https://doi.org/10.1021/acs.est.8b04507Park, S. H., Song, C. B., Kim, M. C., Kwon, S. B., & Lee, K. W. (2004). Study on Size Distribution of Total Aerosol and Water-Soluble Ions During an Asian Dust Storm Event at Jeju Island, Korea. *Environmental Monitoring and Assessment*, *93*(1), 157–183. https://doi.org/10.1023/B:EMAS.0000016805.04194.56Parrish, D. D., Allen, D. T., Bates, T. S., Estes, M., Fehsenfeld, F. C., Feingold, G., et al. (2009). Overview of the Second Texas Air Quality Study (TexAQS II) and the Gulf of Mexico Atmospheric Composition and Climate Study (GoMACCS). *Journal of Geophysical Research*, *114*, D00F13. https://doi.org/10.1029/2009JD011842Pósfai, M., Simonics, R., Li, J., Hobbs, P. V., & Buseck, P. R. (2003). Individual aerosol particles from biomass burning in southern Africa: 1. Compositions and size distributions of carbonaceous particles. *Journal of Geophysical Research: Atmospheres*, *108*(D13), D138483. https://doi.org/10.1029/2002JD002291Putaud, J., Raes, F., Van Dingenen, R., Bruggemann, E., Facchini, M., Decesari, S., et al. (2004). European aerosol phenomenology, 2 : chemical characteristics of particulate matter at kerbside, urban, rural and background sites in Europe. *Atmospheric Environment*, *38*(16), 2579–2595.Rinaldi, M., Decesari, S., Carbone, C., Finessi, E., Fuzzi, S., Ceburnis, D., et al. (2011). Evidence of a natural marine source of oxalic acid and a possible link to glyoxal. *Journal of Geophysical Research*, *116*(D16), D16204. https://doi.org/10.1029/2011JD015659Roberts, G. C., Andreae, M. O., Zhou, J., & Artaxo, P. (2001). Cloud condensation nuclei in the Amazon Basin: "marine" conditions over a continent? *Geophysical Research Letters*, *28*(14), 2807–2810. https://doi.org/10.1029/2000GL012585Saxena, P., & Hildemann, L. M. (1996). Water-soluble organics in atmospheric particles: A critical review of the literature and application of thermodynamics to identify candidate compounds. *Journal of Atmospheric Chemistry*, *24*(1), 57–109. https://doi.org/10.1007/BF00053823Schlosser, J. S., Dadashazar, H., Edwards, E.-L., Mardi, A. H., Prabhakar, G., Stahl, C., et al. (2020). Relationships Between Supermicrometer Sea Salt Aerosol and Marine Boundary Layer Conditions: Insights From Repeated Identical Flight Patterns. *Journal of Geophysical Research: Atmospheres*, *125*(12), e2019JD032346. https://doi.org/10.1029/2019JD032346Schroder, J. C., Campuzano-Jost, P., Day, D. A., Shah, V., Larson, K., Sommers, J. M., et al. (2018). Sources and Secondary Production of Organic Aerosols in the Northeastern United States during WINTER. *Journal of Geophysical Research: Atmospheres*. https://doi.org/10.1029/2018JD028475Sorooshian,

A., Brechtel, F. J., Ma, Y., Weber, R. J., Corless, A., Flagan, R. C., & Seinfeld, J. H. (2006). Modeling and Characterization of a Particle-into-Liquid Sampler (PILS). *Aerosol Science and Technology*, *40*(6), 396–409. https://doi.org/10.1080/02786820600632282Sorooshian, A., Varutbangkul, V., Brechtel, F. J., Ervens, B., Feingold, G., Bahreini, R., et al. (2006). Oxalic acid in clear and cloudy atmospheres: Analysis of data from International Consortium for Atmospheric Research on Transport and Transformation 2004. *Journal of Geophysical Research: Atmospheres*, *111*(D23), D23S45. https://doi.org/10.1029/2005JD006880Sorooshian, A., Lu, M.-L., Brechtel, F. J., Jonsson, H., Feingold, G., Flagan, R. C., & Seinfeld, J. H. (2007). On the Source of Organic Acid Aerosol Layers above Clouds. *Environmental Science & Technology*, *41*(13), 4647–4654. https://doi.org/10.1021/es0630442Sorooshian, A., Ng, N. L., Chan, A. W. H., Feingold, G., Flagan, R. C., & Seinfeld, J. H. (2007). Particulate organic acids and overall water-soluble aerosol composition measurements from the 2006 Gulf of Mexico Atmospheric Composition and Climate Study (GoMACCS). *Journal of Geophysical Research: Atmospheres*, *112*(D13). https://doi.org/10.1029/2007JD008537Sorooshian, A., Padró, L. T., Nenes, A., Feingold, G., McComiskey, A., Hersey, S. P., et al. (2009). On the link between ocean biota emissions, aerosol, and maritime clouds: Airborne, ground, and satellite measurements off the coast of California. *Global Biogeochemical Cycles*, *23*(4), GB4007. https://doi.org/10.1029/2009GB003464Sorooshian, A., Crosbie, E., Maudlin, L. C., Youn, J.-S., Wang, Z., Shingler, T., et al. (2015). Surface and airborne measurements of organosulfur and methanesulfonate over the western United States and coastal areas. *Journal of Geophysical Research: Atmospheres*, *120*(16), 8535–8548. https://doi.org/10.1002/2015JD023822Sorooshian, A., MacDonald, A. B., Dadashazar, H., Bates, K. H., Coggon, M. M., Craven, J. S., et al. (2018). A multi-year data set on aerosol-cloud-precipitation-meteorology interactions for marine stratocumulus clouds. *Scientific Data*, *5*(1), 180026. https://doi.org/10.1038/sdata.2018.26Sorooshian, A., Anderson, B., Bauer, S. E., Braun, R. A., Cairns, B., Crosbie, E., et al. (2019). Aerosol–Cloud–Meteorology Interaction Airborne Field Investigations: Using Lessons Learned from the U.S. West Coast in the Design of ACTIVATE off the U.S. East Coast. *Bulletin of the American Meteorological Society*, *100*(8), 1511–1528. https://doi.org/10.1175/BAMS-D-18-0100.1Sorooshian, A., Corral, A. F., Braun, R. A., Cairns, B., Crosbie, E., Ferrare, R., et al. (2020). Atmospheric Research Over the Western North Atlantic Ocean Region and North American East Coast: A Review of Past Work and Challenges Ahead. *Journal of Geophysical Research: Atmospheres*, *125*(6), e2019JD031626. https://doi.org/10.1029/2019JD031626Stahl, C., Cruz, M. T., Bañaga, P. A., Betito, G., Braun, R. A., Aghdam, M. A., Cambaliza, M. O., Lorenzo, G. R., MacDonald, A. B., Pabroa, P. C., et al. (2020). An annual time series of weekly size-resolved aerosol properties in the megacity of Metro Manila, Philippines. *Scientific Data*, *7*(1), 128. https://doi.org/10.1038/s41597-020-0466-yStahl, C., Cruz, M. T., Bañaga, P. A., Betito, G., Braun, R. A., Aghdam, M. A., Cambaliza, M. O., Lorenzo, G. R., MacDonald, A. B.,

17

Hilario, M. R. A., et al. (2020). Sources and characteristics of size-resolved particulate organic acids and methanesulfonate in a coastal megacity: Manila, Philippines. *Atmospheric Chemistry and Physics*, *20*(24), 15907–15935. https://doi.org/10.5194/acp-20-15907-2020Sullivan, R. C., & Prather, K. A. (2007). Investigations of the Diurnal Cycle and Mixing State of Oxalic Acid in Individual Particles in Asian Aerosol Outflow. *Environmental Science & Technology*, *41*(23), 8062–8069. https://doi.org/10.1021/es071134gŠvédová, B., Kucbel, M., Raclavská, H., Růžičková, J., Raclavský, K., & Sassmanová, V. (2019). Water-soluble ions in dust particles depending on meteorological conditions in urban environment. *Journal of Environmental Management*, *237*, 322–331. https://doi.org/10.1016/j.jenvman.2019.02.086Turekian, V. C., Macko, S. A., & Keene, W. C. (2003). Concentrations, isotopic compositions, and sources of size-resolved, particulate organic carbon and oxalate in near-surface marine air at Bermuda during spring. *Journal of Geophysical Research: Atmospheres*, *108*(D5). https://doi.org/10.1029/2002JD002053Wang, G., Kawamura, K., Cheng, C., Li, J., Cao, J., Zhang, R., et al. (2012). Molecular Distribution and Stable Carbon Isotopic Composition of Dicarboxylic Acids, Ketocarboxylic Acids, and -Dicarbonyls in Size-Resolved Atmospheric Particles From Xi'an City, China. *Environmental Science & Technology*, *46*(9), 4783–4791. https://doi.org/10.1021/es204322cWang, Q., Dong, X., Fu, J. S., Xu, J., Deng, C., Jiang, Y., et al. (2018). Environmentally dependent dust chemistry of a super Asian dust storm in March 2010: observation and simulation. *Atmospheric Chemistry and Physics*, *18*(5), 3505–3521. https://doi.org/10.5194/acp-18-3505-2018Warneck, P. (2003). In-cloud chemistry opens pathway to the formation of oxalic acid in the marine atmosphere. *Atmospheric Environment*, *37*(17), 2423–2427. https://doi.org/10.1016/S1352-2310(03)00136-5Weber, R. J., Orsini, D., Daun, Y., Lee, Y.-N., Klotz, P. J., & Brechtel, F. (2001). A Particle-into-Liquid Collector for Rapid Measurement of Aerosol Bulk Chemical Composition. *Aerosol Science and Technology*, *35*(3), 718–727. https://doi.org/10.1080/02786820152546761Wofsy, S. C., Afshar, S., Allen, H. M., Apel, E. C., Asher, E. C., Barletta, B., et al. (2018). ATom: Merged Atmospheric Chemistry, Trace Gases, and Aerosols. *ORNL DAAC*. https://doi.org/10.3334/ORNLDAAC/1581Wonaschuetz, A., Sorooshian, A., Ervens, B., Chuang, P. Y., Feingold, G., Murphy, S. M., et al. (2012). Aerosol and gas re-distribution by shallow cumulus clouds: An investigation using airborne measurements. *Journal of Geophysical Research: Atmospheres*, *117*(D17), D17202. https://doi.org/10.1029/2012JD018089Yang, F., Gu, Z., Feng, J., Liu, X., & Yao, X. (2014). Biogenic and anthropogenic sources of oxalate in PM2.5 in a mega city, Shanghai. *Atmospheric Research*, *138*, 356–363. https://doi.org/10.1016/j.atmosres.2013.12.006Yao, X., Lau, A. P. S., Fang, M., Chan, C. K., & Hu, M. (2003). Size distributions and formation of ionic species in atmospheric particulate pollutants in Beijing, China: 2—dicarboxylic acids. *Atmospheric Environment*, *37*(21), 3001–3007. https://doi.org/10.1016/S1352-2310(03)00256-5Yao, X., Fang, M., Chan, C. K., Ho, K. F., & Lee, S. C. (2004). Characterization of dicarboxylic acids in PM2.5 in Hong Kong. *Atmospheric Environment*, *38*(7), 963–970.

https://doi.org/10.1016/j.atmosenv.2003.10.048Yu, J. Z., Huang, X.-F., Xu, J., & Hu, M. (2005). When Aerosol Sulfate Goes Up, So Does Oxalate: Implication for the Formation Mechanisms of Oxalate. *Environmental Science & Technology*, *39*(1), 128–133. https://doi.org/10.1021/es049559fZhang, C., Yang, C., Liu, X., Cao, F., & Zhang, Y. (2020). Insight into the photochemistry of atmospheric oxalate through hourly measurements in the northern suburbs of Nanjing, China. *Science of The Total Environment*, *719*, 137416. https://doi.org/10.1016/j.scitotenv.2020.137416Zhang, Q., Jimenez, J. L., Canagaratna, M. R., Allan, J. D., Coe, H., Ulbrich, I., et al. (2007). Ubiquity and dominance of oxygenated species in organic aerosols in anthropogenically-influenced Northern Hemisphere midlatitudes. *Geophysical Research Letters*, *34*(13). https://doi.org/10.1029/2007GL029979Zhang, Qi, Alfarra, M. R., Worsnop, D. R., Allan, J. D., Coe, H., Canagaratna, M. R., & Jimenez, J. L. (2005). Deconvolution and Quantification of Hydrocarbon-like and Oxygenated Organic Aerosols Based on Aerosol Mass Spectrometry. *Environmental Science & Technology*, *39*(13), 4938–4952. https://doi.org/10.1021/es048568lZiemba, L. D., Griffin, R. J., Whitlow, S., & Talbot, R. W. (2011). Characterization of water-soluble organic aerosol in coastal New England: Implications of variations in size distribution. *Atmospheric Environment*, *45*(39), 7319–7329. https://doi.org/10.1016/j.atmosenv.2011.08.022